ELSEVIER

Journal of Organometallic Chemistry 555 (1998) 67–79

Journal of Organometallic Chemistry

Activation of C–F and C–H bonds by polyalkylcyclopentadienylrhodium complexes: crystal structure of $[(\eta^5\text{-}C_5Me_4Et)RhCl\{(C_6F_5)_2PCH_2CH_2P(C_6F_5)_2\}]^+ \cdot BF_4^-$

Malcolm J. Atherton [a], John Fawcett [b], J.H. Holloway [b], Eric G. Hope [b], Sinéad M. Martin [b], David R. Russell [b], Graham C. Saunders [b,*]

[a] *F_2 Chemicals, Springfields, Salwick, Preston PR4 0XJ, UK*
[b] *Department of Chemistry, University of Leicester, Leicester LE1 7RH, UK*

Received 16 September 1997

Abstract

The reaction between $[(\eta^5\text{-}C_5Me_4Et)RhCl(\mu\text{-}Cl)]_2$ and the diphosphine, $(C_6F_5)_2PCH_2CH_2P(C_6F_5)_2$ (dfppe), proceeded via the activation of two C–F and two C–H bonds and the formation of two C–C bonds to give a mixture of isomers of a salt with formulation '$[(\eta^5\text{-}C_5Me_4Et)RhCl\{(C_6F_5)_2PCH_2CH_2P(C_6F_5)_2\}\text{-}2HF]^+ \cdot Cl^-$' (**3a**). Treatment of $[(\eta^5\text{-}C_5Me_4Et)RhCl(\mu\text{-}Cl)]_2$ with NH_4BF_4 followed by dfppe yielded $[(\eta^5\text{-}C_5Me_4Et)RhCl\{(C_6F_5)_2PCH_2CH_2P(C_6F_5)_2\}]^+ \cdot BF_4^-$ (**4b**) which, on thermolysis in ethanol underwent C–F and C–H bond activation to yield the tetrafluoroborate salt of **3a** (**3b**). The structure of **4b** was determined by a single crystal X-ray diffraction study. The salt **4b** crystallizes in the triclinic space group $P\bar{1}$ with $a = 15.743$ (4), $b = 16.429$ (2), $c = 16.970$ (3) Å, $\alpha = 79.41$ (2), $\beta = 84.34$ (2), $\gamma = 82.01$ (2)° and $Z = 4$. Refinement gave final R_1 and $wR^2[I > 2\sigma(I)]$ values of 0.0955 and 0.2200 respectively for 7254 observed reflections. When the reaction between $[(\eta^5\text{-}C_5Me_4Et)RhCl(\mu\text{-}Cl)]_2$ and dfppe was carried out in ethanol, a mixture of **3b**, **4b** and the singly C–F bond activated complex '$[(\eta^5\text{-}C_5Me_4Et)RhCl\{(C_6F_5)_2PCH_2CH_2P(C_6F_5)_2\}\text{–}HF]^+ \cdot BF_4^-$' (**5b**) were obtained after addition of NH_4BF_4. The monophosphines $P(C_6F_5)_3$ and $PPh(C_6F_5)_2$ failed to react with $[(\eta^5\text{-}C_5Me_5)RhCl(\mu\text{-}Cl)]_2$ and the reaction between $[(\eta^5\text{-}C_5Me_5)RhCl(\mu\text{-}Cl)]_2$ and $PPh_2(C_6F_5)$ did not lead to C–F bond activation but yielded $(\eta^5\text{-}C_5Me_5)RhCl_2\{PPh_2(C_6F_5)\}$ (**6**). © 1998 Elsevier Science S.A. All rights reserved.

Keywords: C–F bond activation; C–H bond activation; Rhodium; Crystal Structure; 1,2-Bis{bis(pentafluorophenyl)phosphino}ethane

1. Introduction

The activation of C–F bonds, which are amongst the strongest known, has recently received much attention because of the important applications of functionalized fluorocarbons and the destruction of ozone depleting chlorofluorocarbons [1]. There are a small number of reports of the cleavage of C–F bonds by transition metal complexes [1], but reactions proceeding in high yield under mild conditions are rare [2–9]. Recently, we reported that the fluorinated diphosphine, $(C_6F_5)_2PCH_2CH_2P(C_6F_5)_2$ (dfppe), reacts with $[(\eta_5\text{-}C_5Me_5)RhCl(\mu\text{-}Cl)]_2$ under mild conditions to afford, in quantitative yield, a cationic complex (**1**)[1], in which two aryl C–F bonds and two pentamethylcyclopentadienyl C–H bonds have been cleaved and two C–C bonds have been formed (Eq. (1)) [10,11].

* Corresponding author. Present address: School of Chemistry, The Queen's University of Belfast, David Keir Building, Belfast, BT9 5AG, UK. E-mail: g.saunders@qub.ac.uk

[1] For salts the numbers refer to the cation and the letters indicate the anion: $a = Cl^-$ and $b = BF_4^-$.

PII S0022-328X(97)00704-3

$$1/2[(\eta^5\text{-}C_5Me_5)RhCl(\mu\text{-}Cl)]_2 + (C_6F_5)_2PCH_2CH_2P(C_6F_5)_2 \rightarrow [\{\eta^5\text{-}C_5Me_3[CH_2C_6F_4P(C_6F_5)CH_2]_2\text{-}1,3\}RhCl]^+ \cdot X^- + 2HF (X^- = Cl^-\ \mathbf{1a},\ X^- = BF_4^-\ \mathbf{1b}) \quad (1)$$

The reaction exhibits complete regiospecificity: only one *ortho* C–F bond of each $P(C_6F_5)_2$ moiety and C–H bonds of methyl groups exclusively in a 1,3 disposition are activated. Presumably, this is due solely to geometric constraints. It is significant that there are no anomalous bond distances or angles in the structure of salt **1b** [10]. The arrangement of ligands is such that, when viewed along the C_5(centroid)–Rh axis, the methyl group in the 2 position lies between the two phosphorus atoms and the chloride lies between the 4 and 5 methyl groups (Fig. 1). That geometric constraints determine the geometry of the cation is corroborated by the hydroalkylation of the bisphosphine complex $[(\eta^5\text{-}C_5Me_5)RhCl(PPh_2CH=CH_2)_2]^+ \cdot Cl^-$, which yields $[\{\eta^5\text{-}C_5Me_3(CH_2CH_2CH_2PPh_2)_2\text{-}1,3\}RhCl]^+ \cdot Cl^-$, which possesses a similar arrangement of ligands to that in **1**, as well as the 1,2 isomer [12,13]. The geometry of the dfppe ligand precludes the formation of the 1,2 isomer of **1**. Although intermediates were not observed when reaction (1) was carried out in benzene, when it was performed in ethanol for a shorter time $[(\eta^5\text{-}C_5Me_5)RhCl\{(C_6F_5)_2PCH_2CH_2P(C_6F_5)_2\}]^+$ (**2**) and the singly C–F bond-activated cation $[\{\eta^5\text{-}C_5Me_4CH_2C_6F_4P(C_6F_5)CH_2CH_2P(C_6F_5)_2\}RhCl]^+$, as well as the final product (**1**), were identified in the reaction mixture by mass spectrometry and multinuclear NMR spectroscopies. The complex $[(\eta^5\text{-}C_5Me_5)RhCl\{(C_6F_5)_2PCH_2CH_2P(C_6F_5)_2\}]^+ \cdot BF_4^-$ (**2b**) was prepared independently and C–F bond activation was induced by thermolysis in refluxing ethanol to give **1b** (Eq. (2)) [11].

$$[(\eta^5\text{-}C_5Me_5)RhCl(C_6F_5)_2PCH_2CH_2P(C_6F_5)_2]^+ \cdot BF_4^- \rightarrow [\{\eta^5\text{-}C_5Me_3[CH_2C_6F_4P(C_6F_5)CH_2]_2\text{-}1,3\}RhCl]^+ \cdot BF_4^- + 2HF \quad (2)$$

We are interested in determining the mechanisms of these reactions and whether they are restricted to Eq. (1) and Eq. (2), or whether these are two examples of a more general type of reaction which might prove of great synthetic potential. The [CpMX] system offers scope for investigating and developing this reactivity. The cyclopentadienyl ligand, the metal, the halide and the diphosphine ligand can all be varied to aid in determining the scope of the reaction and elucidating the mechanism. Here, we describe the results obtained on variation of the C–H and C–F bond-containing ligands.

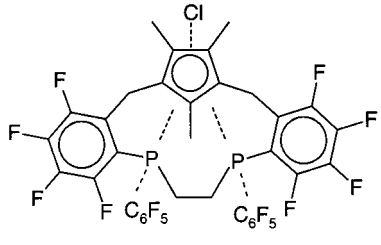

Fig. 1. Diagrammatic representation of the cation $[\{\eta^5\text{-}C_5Me_3[CH_2C_6F_4P(C_6F_5)CH_2]_2\text{-}1,3\}RhCl]^+$ (**1**) viewed along the C_5(centroid)–Rh axis.

The pentamethylcyclopentadienyl ligand possesses only one type of C–H bond which may be activated. The η^5-C_5Me_4Et ligand contains three types of C–H bond; 12 cyclopentadienyl methyl C–H bonds, two methylene C–H bonds and three alkyl methyl C–H bonds. We decided, therefore, to examine whether there is any selectivity in the C–H bond activation by studying the reaction between $[(\eta^5\text{-}C_5Me_4Et)RhCl(\mu\text{-}Cl)]_2$ and dfppe. We have also attempted to activate the C–F bonds of monophosphines containing pentafluorophenyl groups by reaction with $[(\eta^5\text{-}C_5Me_5)RhCl(\mu\text{-}Cl)]_2$.

2. Results and discussion

2.1. Reaction between $[(\eta^5\text{-}C_5Me_4Et)RhCl(\mu\text{-}Cl)]_2$ and dfppe in benzene

Treatment of dfppe with $[(\eta^5\text{-}C_5Me_4Et)RhCl(\mu\text{-}Cl)]_2$ in refluxing benzene for 10.5 h yielded a yellow solution from which was isolated a yellow solid, **3a**. The positive ion FAB mass spectrum shows ions, with associated envelopes at 1005 and 969, consistent with loss of two molecules of HF from the cation $[(\eta^5\text{-}C_5Me_4Et)RhCl\{(C_6F_5)_2PCH_2CH_2P(C_6F_5)_2\}]^+$ and $[M-Cl]^+$. The $^{31}P\{^1H\}$-NMR spectrum, recorded in $CDCl_3$, shows a number of resonances between 72 and 80 ppm which can be assigned as doublets of multiplets with rhodium–phosphorus couplings, $^1J_{Rh-P}$, of magnitude ca. 140 Hz (Fig. 2). These data are comparable with the $^{31}P\{^1H\}$-NMR data for the cation **1** [10]. Thus, the mass spectral and ^{31}P-NMR data indicate that C–F and C–H bond activation and C–C bond formation has occurred and a mixture of cations similar to **1** have been formed. Further evidence for this reaction is provided by the ^{19}F-NMR spectrum of **3a** which shows two resonances at δ −153.73 and −153.78 assigned to the tetrafluoroborate anion, and a singlet at δ −139.77 with ^{28}Si satellites assigned to the hexafluorosilicate dianion. Both are formed by the reaction of evolved HF with the borosilicate glass reaction vessel. Identical resonances have been observed in the products of reaction (1). Furthermore, the negative ion FAB mass spectrum of the crude product shows ions at 86 and 87, assigned to tetrafluoroborate.

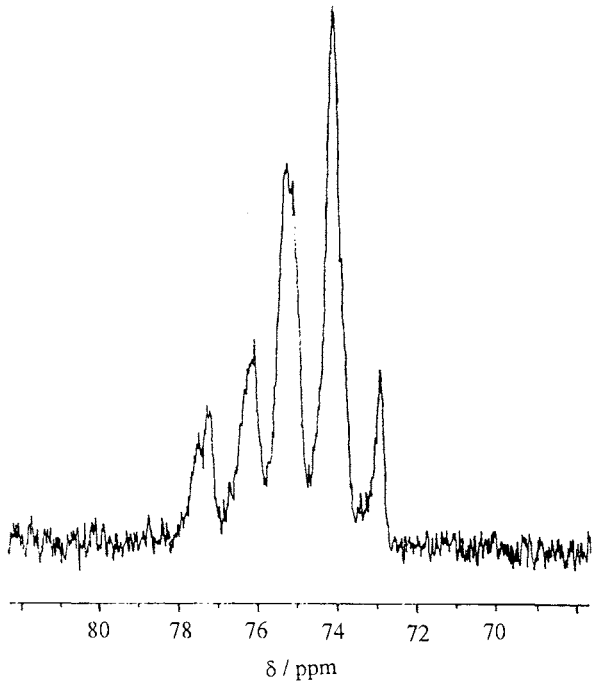

Fig. 2. $^{31}P\{^{1}H\}$ NMR spectrum of '$[(\eta^5\text{-}C_5Me_4Et)RhCl\{(C_6F_5)_2PCH_2CH_2P(C_6F_5)_2\}\text{-}2HF]^+ \cdot Cl^-$' (**3a**).

The ^{1}H- and ^{19}F-NMR spectra of **3a** are consistent with a mixture of isomers of formulation '$[(\eta^5\text{-}C_5Me_4Et)RhCl\{(C_6F_5)_2PCH_2CH_2P(C_6F_5)_2\}\text{-}2HF]^+$'. The ^{1}H-NMR spectrum exhibits several resonances in the region 3–5 ppm, which are assigned to PCH_2 and $C_6F_4CH_2$ methylene hydrogen atoms by analogy with the spectrum of **1a**, and the region 0.9–2.6 ppm, which are assigned to pentaalkylcyclopentadienyl hydrogen atoms. There are a number of distinctive resonances which are presented in Table 1. In particular, a doublet at δ 2.05 dominates the lower frequency region and accounts for over half of the integration of the four doublets between 1.8 and 2.2 ppm. The assignments were made with the aid of the $^{1}H\{^{31}P\}$-NMR spectrum and by analogy with the spectrum of **1a**. It is noted that the resonances of the 4- and 5-methyl group hydrogen atoms are doublets, with coupling to only *one* phosphorus atom. These are consistent with the spectrum of **1a** which exhibits a doublet at δ 2.05 with J_{P-H} 7.3 Hz [10]. These data are, however, different from the ^{1}H spectrum of $[\{\eta^5\text{-}C_5Me_3(CH_2CH_2CH_2PPh_2)_2\text{-}1,3\}RhCl]^+ \cdot PF_6^-$, which exhibits a triplet at δ 1.86 with a coupling of 6.5 Hz assigned to both the 4- and 5-methyl groups [13]. It is also noted that the hydrogen resonances of the methyl groups in the 2-positions of **1a** and **3a** show little or no coupling to phosphorus.

Table 1
Selected ^{1}H NMR data for '$[(\eta^5\text{-}C_5Me_4Et)RhCl\{(C_6F_5)_2PCH_2CH_2P(C_6F_5)_2\}\text{-}2HF]^+ \cdot X^-$' ($X^- = Cl^-$ **3a**, $X^- = BF_4^-$ **3b**)

3a[a]	**3b**[b]	Assignment
1.03 (t, $^{3}J_{H-H} = 7.7$ Hz)	1.22 (t, $^{3}J_{H-H} = 7.4$ Hz)	CH_2CH_3
1.19 (t, $^{3}J_{H-H} = 7.45$ Hz)	1.38 (t, $^{3}J_{H-H} = 7.6$ Hz)	CH_2CH_3
	1.66 (d, $^{3}J_{H-H} = 7.3$ Hz)	$CHCH_3$
	1.79 (d, $^{3}J_{H-H} = 7.4$ Hz)	$CHCH_3$
	1.83 (t, $^{4}J_{P-H} = 2.3$ Hz)	2-CH_3
1.85 (d, $^{4}J_{P-H} \approx 7.5$ Hz)	1.87 (d, $^{4}J_{P-H} = 8.7$ Hz)	4- or 5-CH_3
2.01 (d, $^{4}J_{P-H} \approx 9$ Hz)	2.02 (d, $^{4}J_{P-H} = 7.5$ Hz)	4- or 5-CH_3
2.05 (d, $^{4}J_{P-H} \approx 7$ Hz)	2.07 (d, $^{4}J_{P-H} = 7.3$ Hz)	4- or 5-CH_3
2.13 (d, $^{4}J_{P-H} \approx 5$ Hz)	2.14 (d, $^{4}J_{P-H} = 7.8$ Hz)	4- or 5-CH_3
2.28 (m)	2.32 (m)	CH_2CH_3
2.36 (m)	2.46 (m)	CH_2CH_3

[a] Recorded in $CDCl_3$ at 300.14 MHz.
[b] Recorded in $CDCl_3$ at 400.13 MHz.

The ^{19}F-NMR spectrum, recorded at 298 K and at a spectrometer frequency of 282.41 MHz, exhibits several resonances, consistent with the presence of a mixture of isomers, as well as those assigned to tetrafluoroborate and hexafluorosilicate anions. However, all the isomers possess similar fluorine atom resonances in six regions, all of which can be related to the resonances of **1a**; the *ortho*, *meta* and *para* fluorines of the equivalent C_6F_5 rings and four non-equivalent fluorines of the equivalent C_6F_4 rings. There are six multiplets in the region -115 to -121 ppm, which are assigned to one of the fluorine atoms of each C_6F_4 group. There are broad resonances in the range -126 to -133 ppm, assigned to the *ortho* fluorine atoms of the C_6F_5 rings. The broad nature of these resonances is indicative of hindered rotation about the $P-C_6F_5$ bonds, consistent with that found for **1a**. From -134 to -137 ppm there are four resonances which are assigned to one fluorine atom of each C_6F_4 ring. There are seven resonances between -142 and -146 ppm, which are assigned either to two fluorine atoms of each C_6F_4 group or to one C_6F_4 fluorine atom and the *para* fluorine atoms of the C_6F_5 groups. There are four resonances between -150 and -154 ppm, excluding those assigned to tetrafluoroborate, which are assigned to either the *para* fluorine atoms of the C_6F_5 groups or one fluorine atom of the C_6F_4 groups and between -157 and -161 ppm there are three resonances which are assigned to the *meta* fluorine atoms of the C_6F_5 groups. At higher temperature the spectrum shows little change, except that the *ortho*-C_6F_5 fluorine resonances are considerably sharper. At 218 K there are at least ten resonances assigned to the *ortho*-C_6F_5 fluorine atoms. Integration at higher or lower temperature is consistent with the assignments made by comparison of the spectrum with that of **1a**.

The salt **3a** could not be obtained analytically pure, due to contamination by tetrafluoroborate and hexafluorosilicate anions. However, the tetrafluoroborate salt, **3b**, prepared by anion metathesis with NH_4BF_4 in

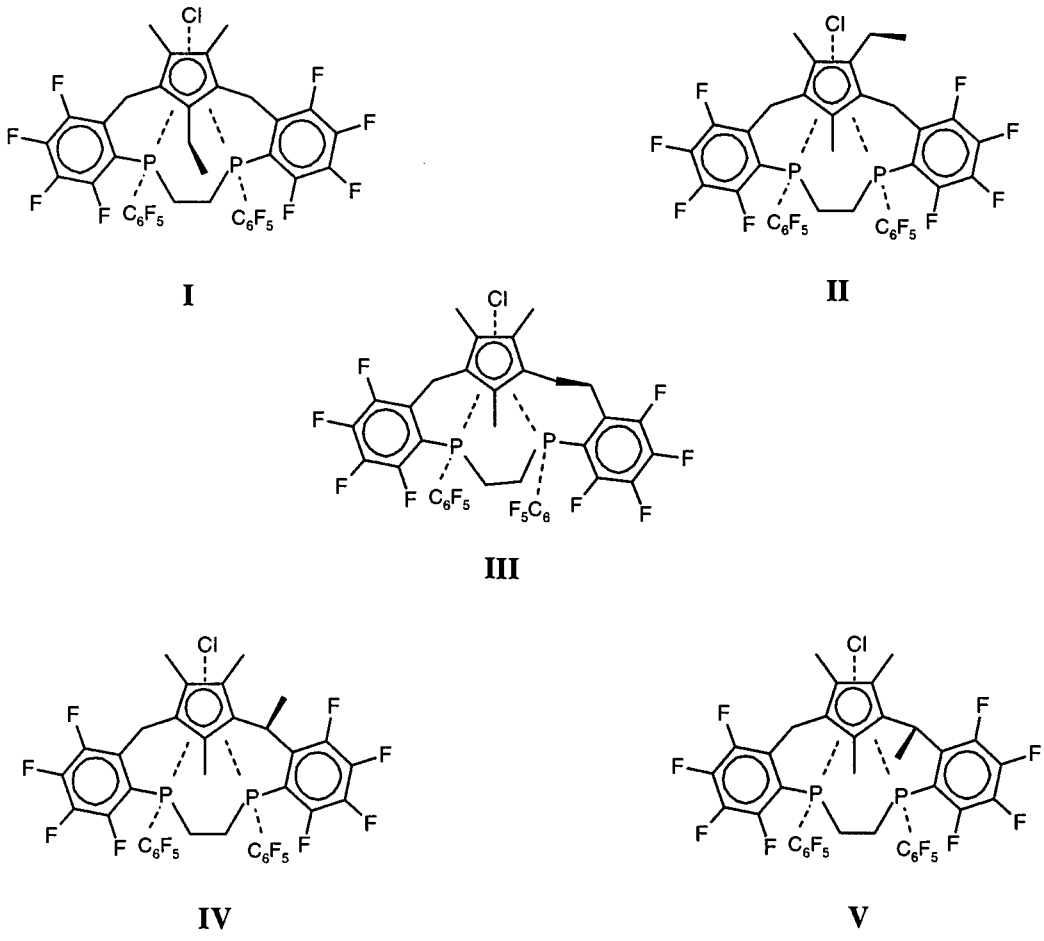

Fig. 3. Diagrammatic representation of the possible isomers of the cation '$[(\eta^5\text{-}C_5Me_4Et)RhCl\{(C_6F_5)_2PCH_2CH_2P(C_6F_5)_2\}\text{-}2HF]^+$' (**3**) viewed along the C_5(centroid)–Rh axes. Isomers **II**–**V** exist as enantiomeric pairs.

methanol, was obtained pure, and characterized by elemental analysis. This confirmed the formulation suggested by the spectroscopic data for **3a**. The positive ion FAB mass spectrum is identical to that of **3a**. The $^{31}P\{^1H\}$-NMR spectrum of **3b** is similar to that of **3a**, exhibiting at least five doublets of multiplets between 70 and 78 ppm with absolute values of $^1J_{Rh-P}$ of 140–150 Hz. The ^{19}F-NMR spectrum of **3b** is also similar to that of **3a**, but with more intense resonances assigned to the tetrafluoroborate anion, no hexafluorosilicate resonance and more resonances in certain regions. In particular, there are five resonances between -150 to -154 ppm. The ^1H-NMR spectrum of **3b**, however, shows significant differences to that of **3a**, although some features are common to both. The prominent features are listed in Table 1. In addition, there are other unassigned resonances in the range 0.9–2.0 ppm and many resonances between 2.8 and 5.0 ppm.

It is reasonable to assume that activation of the C–H bonds occurs at alkyl groups in a 1,3-disposition and that structures similar to those of cation **1** (Fig. 1) and $[\{\eta^5\text{-}C_5Me_3(CH_2CH_2CH_2PPh_2)_2\text{-}1,3\}RhCl]^+$ [12,13] are formed. Thus, there are five possible isomers which are dependent on the position of the C–H bonds are activated (Fig. 3). Isomers **I** and **II** are those expected if activation of only the cyclopentadienyl methyl C–H bonds is occurring, isomer **III** is that expected if one of the C–H bonds of the alkyl methyl group is activated and isomers **IV** and **V** are those expected if one of the methylene C–H bonds is activated. Only isomer **I** possesses the same symmetry as cation **1**, which gives rise to chemical equivalence of the two sides of the cation, and, thus, only one phosphorus resonance, four C_6F_4 fluorine atom resonances and one resonance for both the 4- and 5-methyl hydrogen atoms in the respective NMR spectra. The phosphorus atoms of isomer **I** are chiral, but, as for **1**, only the *meso* stereoisomer can be formed. Isomers **II**–**V** do not possess such symmetry and all the atoms are unique. Thus, two phosphorus resonances and eight C_6F_4 fluorine resonances are expected for each isomer in the ^{31}P- and ^{19}F-NMR spectra respectively. Isomers **II** and **III** contain three chiral centres, namely, both phosphorus atoms and the rhodium atom. However, because of the geometry of the cation, only one pair of enantiomers can exist for each. Isomers **IV** and **V** contain four chiral centres:

both phosphorus atoms, the rhodium atom and the $C_5\underline{C}HMeC_6F_4$ carbon atom. Isomer **V** is that formed by epimerization of **IV** at this carbon. One pair of enantiomers exists for both **IV** and **V**. The presence of two sets of resonances assigned to the methylene and methyl hydrogen atoms of the ethyl group indicates that both **I** and **II** are formed, whilst the presence of two resonances assigned to the methyl hydrogen atoms of $CHCH_3$ groups indicates that **IV** and **V** are also formed. The resonances of the $C_5C\underline{H}MeC_6F_4$ hydrogen atoms of these isomers presumably occur in the region where the resonances for PCH_2 and $C_5CH_2C_6F_4$ occur and cannot be distinguished. The presence of isomers **I**, **II**, **IV** and **V** in **3a** and **3b** should give rise to seven doublets of multiplets in the $^{31}P\{^1H\}$-NMR spectra and seven resonances in the region -115 to -121 ppm in the ^{19}F-NMR spectra. Presumably, resonances are coincidental in the observed spectra. As well as the ^1H-NMR resonances already discussed, there should be six doublets for isomers **I**, **II**, **IV** and **V** assigned to the 4- and 5-methyl hydrogen atoms and three singlets, or triplets with small coupling, assigned to the 2-methyl hydrogen atoms. The ^1H-NMR spectra of both **3a** and **3b** show four prominent doublets (Table 1) and, although no singlets assigned to the 2-methyl group can be discerned in the spectrum of **3a**, that of **3b** does show a prominent triplet at δ 1.83 and a singlet at δ 1.29. The other expected resonances may be obscured. There are no resonances which can be assigned unequivocally to isomer **III**, but this does not necessarily indicate its absence. Unfortunately, due to the NMR spectra containing coincidental and obscured resonances, it is not possible to determine the relative proportions of the isomers of **3a** or **3b** by integration. Attempts to separate the isomers by fractional crystallization and grow crystals suitable for single-crystal X-ray diffraction were unsuccessful.

2.2. Reaction between $[(\eta^5\text{-}C_5Me_4Et)RhCl(\mu\text{-}Cl)]_2$ and dfppe in ethanol

The reaction between $[(\eta^5\text{-}C_5Me_4Et)RhCl(\mu\text{-}Cl)]_2$ and dfppe was also carried out in ethanol, but, as with the reaction between $[(\eta^5\text{-}C_5Me_5)RhCl(\mu\text{-}Cl)]_2$ and dfppe [11], was halted after 2 h. in order to identify any intermediates. The $^{31}P\{^1H\}$-NMR of the mixture, recorded in $(CD_3)_2CO$, shows a number of doublets of multiplets (Fig. 4). The resonance at δ 28.7 shows a rhodium–phosphorus coupling, $^1J_{Rh-P}$, of 152 Hz and is assigned to $[(\eta^5\text{-}C_5Me_4Et)RhCl\{(C_6F_5)_2PCH_2CH_2P(C_6F_5)_2\}]^+$ (**4**) by comparison with the $^{31}P\{^1H\}$-NMR spectrum of $[(\eta^5\text{-}C_5Me_5)RhCl\{(C_6F_5)_2PCH_2CH_2P(C_6F_5)_2\}]^+ \cdot BF_4^-$ [11] and $[(\eta^5\text{-}C_5Me_4Et)RhCl\{(C_6F_5)_2PCH_2CH_2P(C_6F_5)_2\}]^+ \cdot BF_4^-$ (**4b**) (see Section 2.3). There are at least three doublets of multiplets in the range 40–45 ppm with values of $^1J_{Rh-P}$ of ca. 150 Hz, and similar resonances in the range 75–80 ppm. These can be assigned to a mixture of isomers of a cation of formulation '$[(\eta^5\text{-}C_5Me_4Et)RhCl\{(C_6F_5)_2PCH_2CH_2P(C_6F_5)_2\}\text{-}HF]^+$' (**5**) by comparison with the $^{31}P\{^1H\}$-NMR data of $[\{\eta^5\text{-}C_5Me_4CH_2C_6F_4\text{-}P(C_6F_5)CH_2CH_2P(C_6F_5)_2\}RhCl]^+ \cdot BF_4^-$ [11]. The lower frequency resonances are assigned to the $P(C_6F_5)_2$ phosphorus atoms and those at higher frequency to the $CH_2C_6F_4P(C_6F_5)$ phosphorus atoms. There are also less intense resonances at ca. δ 75 which are assigned to the product cation **3**, and two doublets of multiplets at δ 19.0 and 49.2 with values of $^1J_{Rh-P}$ of 62 and 119 Hz respectively, which are due to unidentified compounds. After anion metathesis with NH_4BF_4 a yellow solid was obtained, the FAB mass spectrum of which corroborates the ^{31}P-NMR data. There are peaks with associated envelopes at 1045 and 1010, which are indicative of the cation **4** and [**4**–Cl] respectively, and at 1025 and 989, which correspond to the cation **5** and [**5**–Cl]. There are also less intense peaks centred at 1005 and 969 which are characteristic of the cation **3**. Thus, as with $[(\eta^5\text{-}C_5Me_5)RhCl(\mu\text{-}Cl)]_2$, intermediate species are observed in the reaction carried out in ethanol. The adduct cation **4** is formed initially, and stepwise C–F and C–H bond activation/C–C bond formation affords **5** and then **3** (Scheme 1).

There are seven possible isomers of the cation **5**, dependent on which C–H bond is activated (Fig. 5). Each isomer exists as an enantiomeric pair. The presence of at least three pairs of doublets of multiplets in the $^{31}P\{^1H\}$-NMR spectrum indicates that at least three of these are formed, but does not preclude the formation of the other four since resonances may be obscured and the rate of the reactions may be such that only small amounts of particular isomers of **5** may be present. Table 2 details the resulting isomers of the final product **3** from the isomers of the intermediate **5**, assuming that the Rh–P bonds are not broken during the reaction. It is not possible to determine from the $^{31}P\{^1H\}$-NMR spectrum the selectivity in terms of

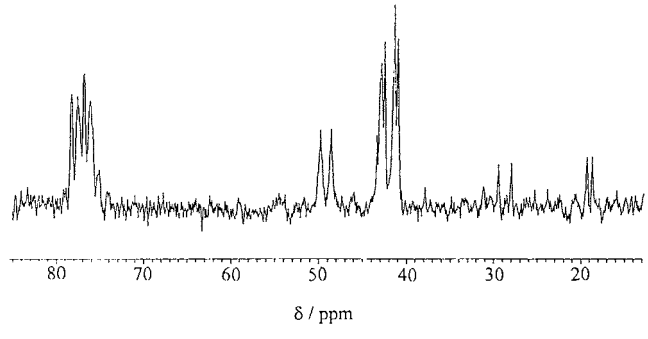

Fig. 4. $^{31}P\{^1H\}$ NMR spectrum, in $(CD_3)_2CO$, of the mixture of products obtained in the reaction between $[(\eta^5\text{-}C_5Me_4Et)RhCl(\mu\text{-}Cl)]_2$ and dfppe in ethanol after 2 h.

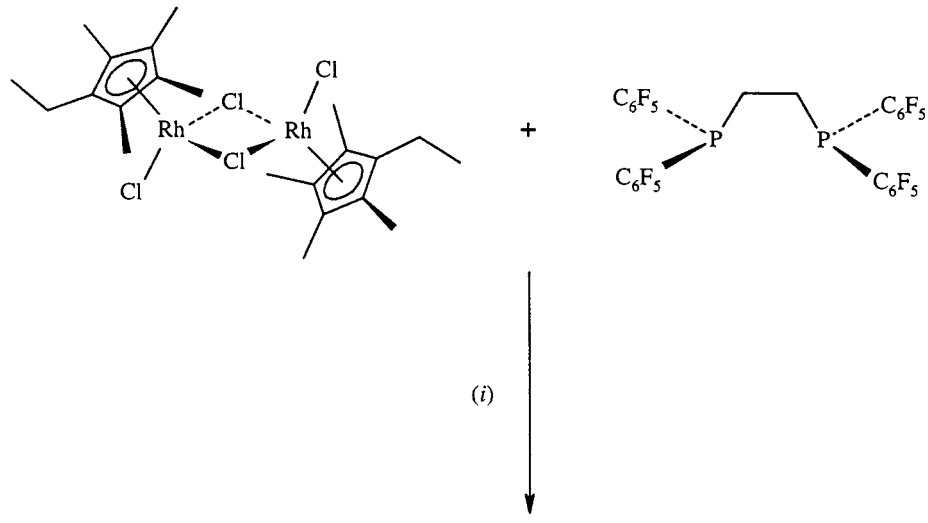

"$[(\eta^5\text{-}C_5Me_4Et)RhCl\{(C_6F_5)_2PCH_2CH_2P(C_6F_5)_2\}$ - 2HF]+" BF_4^- **3b**

Scheme 1. (i) benzene, heat.

which C–H bonds are cleaved first, but it is noted that isomers **VI**–**IX** are formed by the activation of similar cyclopentadienyl methyl C–H bonds and subsequent reaction of these can lead to all the isomers of **3**.

2.3. Synthesis and characterization of $[(\eta^5\text{-}C_5Me_4Et)RhCl\{(C_6F_5)_2PCH_2CH_2P(C_6F_5)_2\}]^+ \cdot BF_4^-$ (4b)

Treatment of $[(\eta^5\text{-}C_5Me_4Et)RhCl(\mu\text{-}Cl)]_2$ with NH_4BF_4 in methanol, followed by addition of dfppe in dichloromethane, afforded the air-stable, orange complex $[(\eta^5\text{-}C_5Me_4Et)RhCl\{(C_6F_5)_2PCH_2CH_2P(C_6F_5)_2\}]^+ \cdot BF_4^-$ (**4b**) in moderate yield (Scheme 2). The complex was characterized by mass spectrometry and NMR spectroscopies. Elemental analysis indicated that it was contaminated with small amounts of C–F bond activated compounds. The mass spectrum exhibited the parent cation at 1045. The ^{1}H-NMR spectrum, recorded in $(CD_3)_2CO$, exhibits two multiplets at δ 3.40 and 1.77 with intensities 4:12 assigned to the PCH_2 and the cyclopentadienyl methyl hydrogen atoms respectively, and a quartet at δ 2.33 and a triplet at δ 1.31 with intensities 2:3 assigned to the methylene and methyl hydrogen atoms of the ethyl group respectively. The $^{31}P\{^1H\}$-NMR spectrum of **4b** exhibits a doublet of multiplets at δ 34.2 with an absolute value of $^1J_{Rh-P}$ of 152 Hz. These values are similar to those of δ 35.1 and 150.5 Hz for complex **2b** [11]. The ^{19}F-NMR spectrum exhibits six resonances assigned to two pairs of *ortho*, *meta* and *para* fluorine atoms, consistent with non-equivalent C_6F_5 groups on each phosphorus atom, as well as resonances assigned to the tetrafluoroborate anion. The values of δ are almost identical to those of **2b** [11]. One of the *ortho* resonances is broadened by hindered rotation about the P–C bonds, as has been found for **2b**.

2.4. Crystal structure of $[(\eta^5\text{-}C_5Me_4Et)RhCl\{(C_6F_5)_2PCH_2CH_2P(C_6F_5)_2\}]^+ \cdot BF_4^-$ (4b)

The structure of complex **4b** has been determined by a single-crystal X-ray diffraction study. The crystallographic data and atomic coordinates are given in Tables 3 and 4, respectively and selected interatomic distances and angles are given in Table 5. The asymmetric unit consists of two unique ion pairs, which are similar in structure (Fig. 6). Both cations exhibit a three-legged piano stool geometry, similar to that adopted by the cation of **2b** [11]. One cation of **4b** possesses P–Rh–Cl angles which are similar, whilst the angles of the other differ by over 10°. The P–Rh–P angles of both cations are similar and ca. 1° more acute than that of **2b** [84.05(8)°]. The Rh–Cl distances are the same as that of **2b** [2.380(2) Å] within experimental error. Three of the Rh–P distances are similar to the shorter Rh–P distance in **2b** [2.342(2) Å], but one is longer by ca. 0.04 Å. The P–CH_2 and CH_2–CH_2 bond lengths are identical to those of **2b** within experimental error, but the P–C_6F_5 bonds are up to 0.03 Å longer than those of **2b**. Each cation of **4b** possesses one smaller and one larger Rh–P–CH_2 angle of ca. 105° and ca. 110°, respectively, consistent with the structure of **2b**. The P–CH_2–CH_2 angles lie in the range 111.3(9)–112.9(10)°. For each phosphorus atom there is

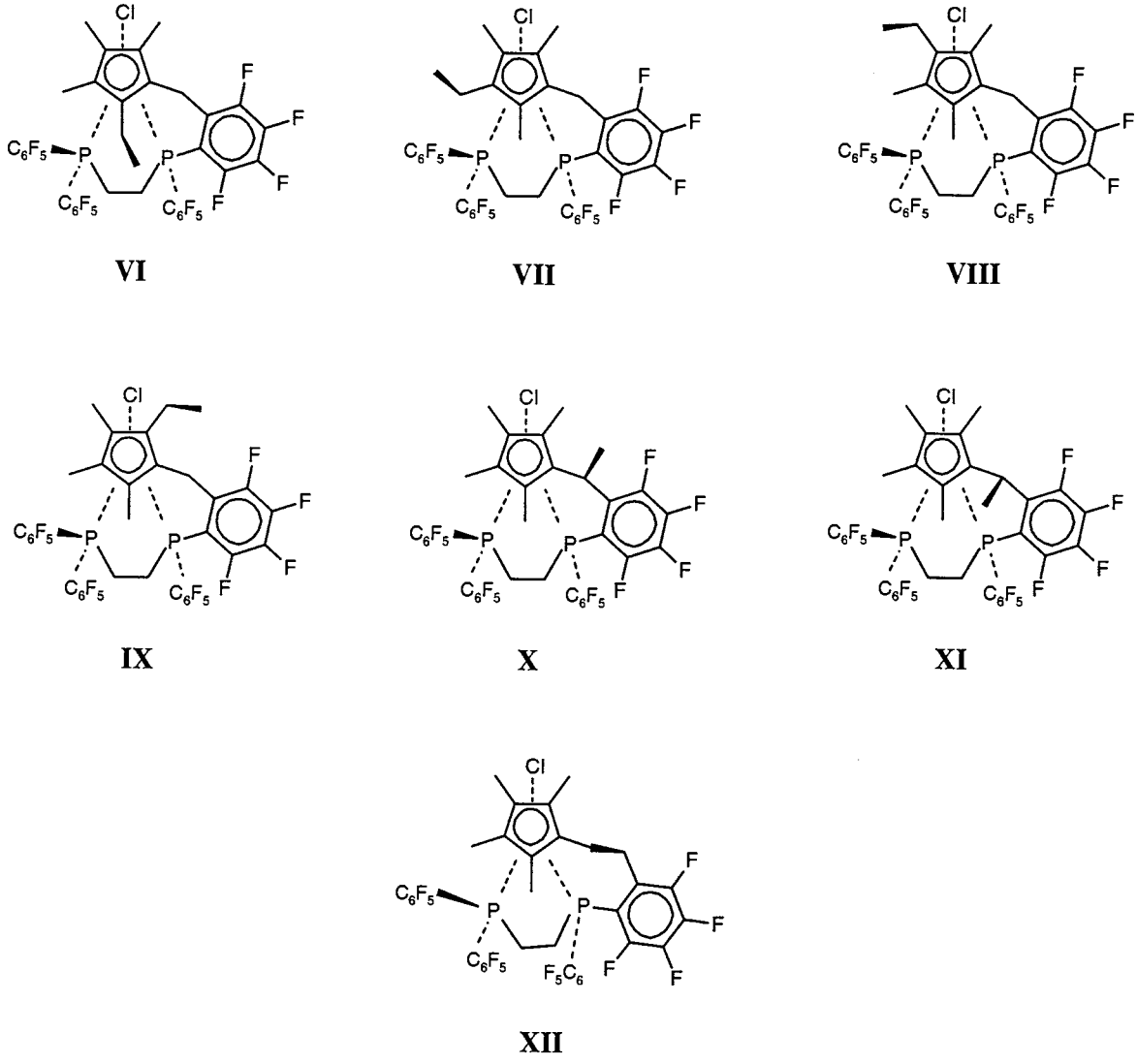

Fig. 5. Diagrammatic representation of the possible isomers of the cation '$[(\eta^5\text{-}C_5Me_4Et)RhCl\{(C_6F_5)_2PCH_2CH_2P(C_6F_5)_2\}\text{-}HF]^+$' (**5**) viewed along the C_5(centroid)-Rh axes. All the isomers exist as enantiomeric pairs.

one smaller Rh–P–C_6F_5 angle of 111.3(5)–117.7(5)° and one larger angle of 123.1(5)–128.5(5)°.

There are a number of short F···C(methyl) distances between the ethyltetramethylcyclopentadienyl ring and the dfppe ligand. In particular, the interatomic distances of 2.910(19) and 2.997(17) Å for C(10)···F(42) and C(11A)···F(32A), respectively are >0.1 Å less than the sum of the van der Waals' radii (3.17 Å) [14]. These distances are shorter by ca. 0.1 Å than analogous distances in the structure of salt **2b**. This may be due to the increased steric pressure of the ethyl group compared to that of a methyl group. The ethyl groups adopt positions such that they are almost eclipsed with the chlorides, the least bulky ligands, when viewed along the C_5(centroid)–Rh axes, and the ethyl CH_3 group is positioned on the other side of the cyclopentadienyl ring to the rhodium atom. There are also a number of F···H distances which are calculated to be significantly less than the sum of the van der Waals' radii (2.67 Å) [14]: F(42)···HC(10) 2.074(18), F(36)···HC(13) 2.238(20), F(32A)···HC(11A) 2.243(17) and F(26A)···HC(11A) 2.265(20) Å. Each tetrafluoroborate anion is situated above the respective cyclopenta-

Table 2
Possible isomers of cations **3** and **5** formed in the reaction between $[(\eta^5\text{-}C_5Me_4Et)RhCl(\mu\text{-}Cl)]_2$ and dfppe

Intermediate **5**→	Product **3**
VI	**I**
VII	**III**, **IV** or **V**
VIII	**II**
IX	**II**
X	**IV**
XI	**V**
XII	**III**

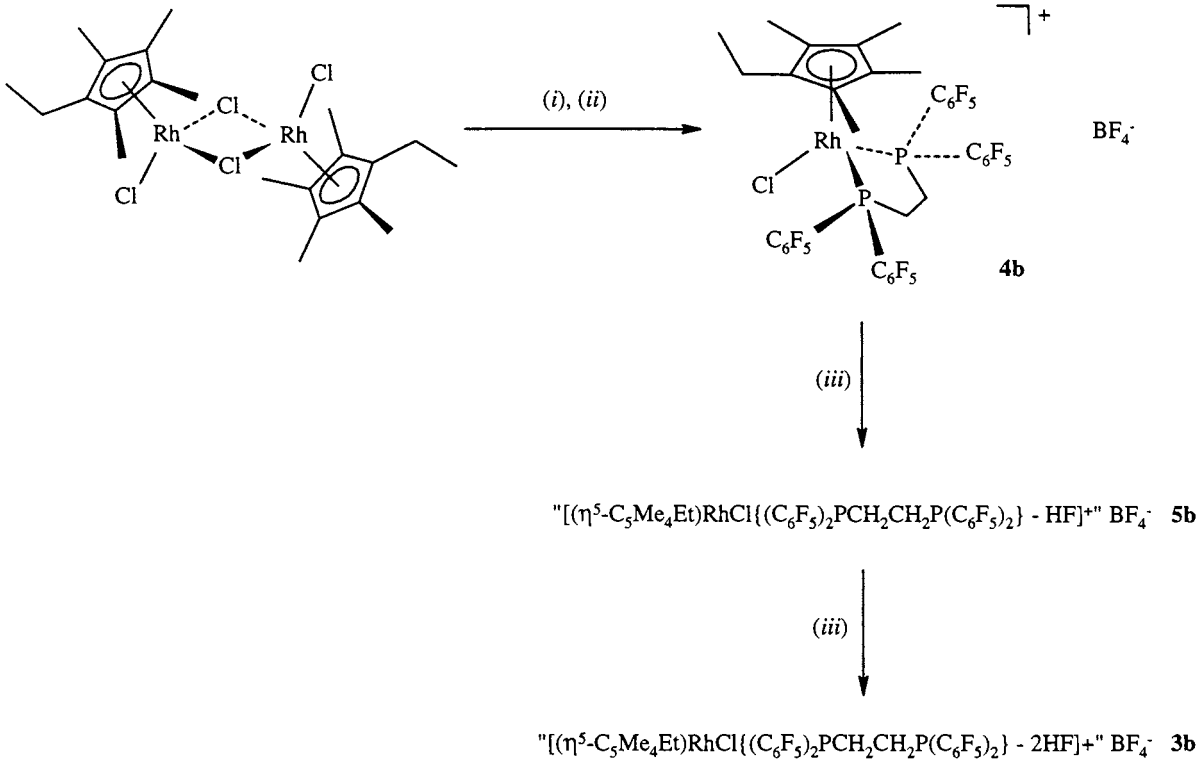

Scheme 2. (i) NH_4BF_4, methanol; (ii) dfppe, dichloromethane; (iii) ethanol, heat.

dienyl ring such that three fluorine atoms of the anion are almost coplanar with the ring. The plane defined by F(1), F(3/3′) and F(4/4′) is ca. 15.0° from planarity with the plane defined by C(3A), C(4A), C(5A), C(6A) and C(7A) and the plane defined by F(6/6′), F(7/7′) and F(8/8′) is ca. 7.4° from planarity with the plane defined by C(3), C(4), C(5), C(6) and C(7). The separation between the two planes at the centroid of the BF_3 base for both salts is ca. 3.2 Å, which is similar to that found for **2b**. The deviations form planarity, however, are greater than that of 5.1° for **2b**, which may be a consequence of the presence of the ethyl group.

2.5. Thermolysis of $[(\eta^5\text{-}C_5Me_4Et)RhCl\{(C_6F_5)_2PCH_2CH_2P(C_6F_5)_2\}]^+ \cdot BF_4^-$ (4b)

Thermolysis of **4b** in refluxing ethanol for 6 h. afforded an orange solid. The FAB mass spectrum shows ions at 1005 and 969, consistent with cation **3**. Thus, C–F and C–H bond activation and C–C bond formation has occurred. The ^1H and ^{19}F-NMR spectra of the product, recorded in $CDCl_3$, are similar to those of **3b**, confirming the conclusion drawn from the mass spectral data, but also contain some extra resonances of low intensity. The $^{31}P\{^1H\}$-NMR spectrum exhibits prominent doublets of multiplets at δ 70.7, 72.4 and 74.0 with couplings, $^1J_{Rh-P}$, of 145, 145 and 140 Hz respectively, which are assigned to isomers of **3b**. Other resonances may be present but are obscured or coincidental. The relative intensities of the resonances of **3b** formed by this route are the same as those found in the reactions between $[(\eta^5\text{-}C_5Me_4Et)RhCl(\mu\text{-}Cl)]_2$ and dfppe. The $^{31}P\{^1H\}$-NMR spectrum also exhibits less intense doublets of multiplets at δ 41.4, 43.2, 75.2 and 77.1 with couplings, $^1J_{Rh-P}$, of 152, 153, ca. 140 and 148 Hz. These can be assigned to singly C–F bond activated species of formulation '$[(\eta^5\text{-}C_5Me_4Et)RhCl\{(C_6F_5)_2PCH_2CH_2P(C_6F_5)_2\}\text{-}HF]^+ \cdot BF_4^-$' (**5b**) by comparison with the $^{31}P\{^1H\}$-NMR spectrum of $[\{\eta^5\text{-}C_5Me_4\text{-}CH_2C_6F_4P(C_6F_5)CH_2CH_2P(C_6F_5)_2\}RhCl]^+ \cdot BF_4^-$ [11]. The mass spectrum also shows peaks at 1025 and 990 which are consistent with this cation and $[M-Cl]^+$.

2.6. Reactions between $[(\eta^5\text{-}C_5Me_5)RhCl(\mu\text{-}Cl)]_2$ and $PPh_x(C_6F_5)_{3-x}$ $(x = 0–2)$

Treatment of $[(\eta^5\text{-}C_5Me_5)RhCl(\mu\text{-}Cl)]_2$ with $PPh_2(C_6F_5)$ in either refluxing ethanol or benzene yielded the neutral complex $(\eta^5\text{-}C_5Me_5)RhCl_2\{PPh_2\text{-}(C_6F_5)\}$ (**6**) (Scheme 3). There is no evidence of C–F bond activation occurring in either solvent, even on prolonged reflux. Complex **6** is a red, air-stable solid, which was characterized by elemental analysis,

mass spectrometry and NMR spectroscopies. The ^{1}H-NMR spectrum, recorded in $CDCl_3$, exhibits two multiplets between 7.2 and 8.0 ppm assigned to the aromatic hydrogen atoms and a doublet at δ 1.30 with a phosphorus–hydrogen coupling, $4J_{P-H}$, of 2.2 Hz assigned to the pentamethylcyclopentadienyl hydrogen atoms. The $^{31}P\{^1H\}$-NMR spectrum exhibits a doublet of multiplets centred at δ 18.8 with a value of $^1J_{Rh-P}$ of 149 Hz. These values may be compared with those of δ 7.9 and 144 Hz for $(\eta^5\text{-}C_5Me_5)RhCl_2(PPh_3)$ [15]. No reaction was observed on treatment of $[(\eta^5\text{-}C_5Me_5)RhCl(\mu\text{-}Cl)]_2$ with either $PPh(C_6F_5)_2$ or $P(C_6F_5)_3$ in refluxing benzene. Presumably, the bulky nature of these ligands prevents their coordination to the rhodium centre. An attempt to prepare the bisphosphine cationic complex $[(\eta^5\text{-}C_5Me_5)RhCl\{PPh_2(C_6F_5)\}_2]^+ \cdot BF_4^-$ by treatment of $[(\eta^5\text{-}C_5Me_5)RhCl(\mu\text{-}Cl)]_2$ with NH_4BF_4 and $PPh_2(C_6F_5)$ was unsuccessful and yielded only complex **6**. Presumably, $PPh_2(C_6F_5)$ is too bulky to permit coordination of two phosphines to the rhodium.

Table 3
Crystallographic data for $[(\eta^5\text{-}C_5Me_4Et)RhCl\{(C_6F_5)_2PCH_2\text{-}CH_2P(C_6F_5)_2\}]^+ \cdot BF_4^- \cdot \{(CH_3)_2CO\}_{0.25}$ (**4b**$\cdot\{(CH_3)_2CO\}_{0.25}$)

Formula	$C_{37.75}H_{22.50}BClF_{24}O_{0.25}P_2Rh$
Formula weight	1147.17
Crystal system	Triclinic
Space group	$P\bar{1}$
Unit cell dimension	
a (Å)	15.743(4)
b (Å)	16.429(2)
c (Å)	16.970(3)
α (°)	79.41(2)
β (°)	84.34(2)
γ (°)	82.01(2)
V (Å^3)	4260.5(14)
Z	4[a]
F(000)	2256
D_c (g cm^{-3})	1.793
Crystal size (mm)	$0.65 \times 0.09 \times 0.08$
Radiation (λ, Å)	Mo-K$_\alpha$ (0.71073)
Monochromator	Graphite
μ (Mo–K$_\alpha$), cm^{-1}	6.75
T (K)	293
Scan method	ω
h, k, l ranges	−1–18, −19–19, −20–19
2θ limits (°)	5.0–50.0
Total reflections	14708
Unique reflections	13137 ($R_{int} = 0.0536$)
Observed reflections $[F_o > 4\sigma(F_o)]$	7254
Restraints	13
Variables	1171
R_1, wR^2 [I $> 2\sigma$(I)]	0.0955, 0.2200
R_1, wR^2 (all data)	0.1757, 0.2714
Weighting scheme	$w = 1/[\sigma^2(F_o)^2 + 0.1279P^2 + 55.10P]$[b]
$(\Delta/\sigma)_{max}$	0.087
max, min $\Delta\rho$ (eÅ^{-3})	0.923, −0.889
Goodness of fit on F^2	1.060

[a] There are two independent ion pairs in the asymmetric unit.
[b] $P = [\max(F_o^2, 0) + 2F_c^2]/3$

Table 4
Atomic coordinates ($\times 10^4$) and equivalent isotropic displacement coefficients (Å$^2 \times 10^3$) with estimated standard deviations in parentheses for the non-hydrogen atoms of $[(\eta^5\text{-}C_5Me_4Et)RhCl\{(C_6F_5)_2PCH_2\text{-}CH_2P(C_6F_5)_2\}]^+ \cdot BF_4^- \cdot \{(CH_3)_2CO\}_{0.25}$ (**4b**$\cdot\{(CH_3)_2CO\}_{0.25}$)

Atom	x	y	z	$U_{(eq)}$
Rh(1)	2926(1)	2640(1)	8897(1)	34(1)
Cl(1)	2679(3)	2495(2)	10321(2)	49(1)
P(1)	2810(2)	1207(2)	9119(2)	36(1)
P(2)	4390(2)	2166(2)	9143(2)	34(1)
C(1)	3806(9)	619(8)	9491(9)	39(3)
C(2)	4353(9)	1165(8)	9807(8)	41(3)
C(3)	2174(10)	3917(8)	8796(9)	44(4)
C(4)	2884(10)	3974(8)	8217(9)	45(4)
C(5)	2852(9)	3410(8)	7685(7)	38(3)
C(6)	2053(9)	3038(8)	7905(9)	43(4)
C(7)	1677(10)	3325(9)	8604(9)	45(4)
C(8)	1347(17)	5238(15)	9086(16)	136(11)
C(9)	1923(12)	4445(9)	9425(10)	63(5)
C(10)	3473(11)	4656(9)	8094(10)	59(4)
C(11)	3374(10)	3375(9)	6898(8)	54(4)
C(12)	1685(10)	2578(9)	7390(9)	54(4)
C(13)	808(10)	3174(11)	9010(11)	70(5)
C(21)	2690(9)	618(8)	8311(8)	40(3)
C(22)	3180(10)	823(9)	7589(9)	46(4)
C(23)	3207(12)	396(11)	6964(10)	59(5)
C(24)	2722(12)	−257(11)	7045(12)	66(5)
C(25)	2266(10)	−497(10)	7760(12)	60(5)
C(26)	2272(10)	−69(10)	8383(10)	52(4)
F(22)	3702(6)	1421(5)	7494(5)	62(2)
F(23)	3691(7)	591(6)	6295(5)	80(3)
F(24)	2742(8)	−691(8)	6452(7)	107(4)
F(25)	1833(7)	−1141 (7)	7855(8)	106(4)
F(26)	1844(6)	−364(6)	9090(7)	76(3)
C(31)	1913(9)	943(9)	9877(8)	43(4)
C(32)	2012(10)	700(9)	10672(10)	51(4)
C(33)	1323(15)	609(14)	11236 (10)	85(7)
C(34)	505(15)	727(15)	11001 (12)	90(7)
C(35)	398(11)	963(13)	10219 (12)	73(5)
C(36)	1077(11)	1046(9)	9649(9)	53(4)
F(32)	2806(7)	533(6)	10969(5)	73(3)
F(33)	1456(9)	362(9)	12025(6)	119(5)
F(34)	−150(9)	620(13)	11543 (8)	162(7)
F(35)	−388(7)	1084(9)	9936(8)	111(4)
F(36)	939(5)	1270(6)	8880(5)	61(2)
C(41)	5141(9)	2001(9)	8281(8)	40(3)
C(42)	5281(10)	2690(9)	7705(9)	48(4)
C(43)	5742(11)	2660(11)	6982(9)	57(4)
C(44)	6105(12)	1924(13)	6811(12)	70(5)
C(45)	6036(12)	1195(11)	7371(12)	67(5)
C(46)	5549(10)	1259(10)	8093(9)	52(4)
F(42)	4972(6)	3447(5)	7864(5)	62(2)
F(43)	5822(8)	3354(7)	6448(6)	93(4)
F(44)	6580(9)	1857(8)	6109(7)	114(4)
F(45)	6434(8)	467(7)	7235(8)	105(4)
F(46)	5524(7)	541(6)	8613(6)	75(3)
C(51)	5023(10)	2690(9)	9688(8)	44(4)
C(52)	4764(10)	3398(9)	9987(9)	45(4)
C(53)	5245(11)	3717(9)	10457(9)	54(4)
C(54)	6053(12)	3333(11)	10623(10)	60(5)
C(55)	6371(11)	2611(10)	10341(10)	56(4)
C(56)	5865(9)	2298(9)	9883(8)	43(4)
F(52)	3991(6)	3819(5)	9852(5)	58(2)
F(53)	4958(7)	4415(6)	10765(6)	78(3)
F(54)	6525(8)	3632(7)	11084(7)	92(4)

Table 4 (*Continued*)

Atom	*x*	*y*	*z*	$U_{(eq)}$
F(55)	7151(6)	2228(6)	10482(7)	83(3)
F(56)	6206(6)	1596(5)	9600(5)	59(2)
Rh(2)	2772(1)	2768(1)	13905(1)	35(1)
Cl(2)	2665(3)	2502(2)	15333(2)	50(1)
P(3)	1307(2)	2596(2)	14174(2)	39(1)
P(4)	2248(2)	4175(2)	13899(2)	38(1)
C(1A)	841(10)	3434(8)	14712(9)	50(4)
C(2A)	1133(9)	4269(9)	14336(9)	46(4)
C(3A)	4120(10)	2163(9)	13931(9)	47(4)
C(4A)	3580(10)	1602(9)	13755(8)	44(4)
C(5A)	3275(8)	1939(9)	12998(7)	37(3)
C(6A)	3538(9)	2753(9)	12731(8)	42(4)
C(7A)	4097(9)	2861(9)	13303(8)	41(3)
C(8A)	5531(15)	1490(16)	14391(13)	117(9)
C(9A)	4681(11)	1997(11)	14614(10)	66(5)
C(10A)	3499(12)	746(9)	14222(10)	62(5)
C(11A)	2872(11)	1466(9)	12484(9)	54(4)
C(12A)	3395(12)	3271(10)	11941(8)	57(4)
C(13A)	4681(10)	3513(11)	13172(10)	62(5)
C(21A)	1138(10)	1616(9)	14828(8)	46(4)
C(22A)	898(9)	1484(10)	15653(9)	53(4)
C(23A)	722(11)	718(11)	16127(10)	59(4)
C(24A)	873(14)	33(12)	15739(15)	84(7)
C(25A)	1122(12)	130(11)	14944(13)	68(5)
C(26A)	1193(10)	889(9)	14513(10)	49(4)
F(22A)	730(7)	2136(6)	16053(5)	69(3)
F(23A)	575(7)	662(7)	16902(6)	92(4)
F(24A)	762(9)	−711(7)	16195(8)	114(4)
F(25A)	1187(8)	−551(6)	14591(8)	101(4)
F(26A)	1388(6)	931(5)	13738(6)	66(3)
C(31A)	495(10)	2620(9)	13452(9)	45(4)
C(32A)	684(11)	2791(10)	12624(11)	59(4)
C(33A)	54(17)	2875(11)	12088(11)	79(6)
C(34A)	−764(15)	2765(12)	12376(14)	77(6)
C(35A)	−971(12)	2587(12)	13207(14)	79(6)
C(36A)	−360(12)	2523(10)	13710(12)	64(5)
F(32A)	1477(7)	2913(7)	12315(6)	80(3)
F(33A)	280(8)	3015(8)	11298(7)	106(4)
F(34A)	−1362(9)	2830(8)	11856(9)	122(5)
F(35A)	−1772(7)	2503(8)	13460(8)	104(4)
F(36A)	−573(6)	2362(6)	14504(7)	73(3)
C(41A)	2712(10)	4856(8)	14454(8)	39(3)
C(42A)	3440(10)	4624(9)	14877(9)	49(4)
C(43A)	3728(12)	5156(10)	15317(9)	57(4)
C(44A)	3272(13)	5947(12)	15297(10)	66(5)
C(45A)	2590(12)	6180(10)	14868(10)	56(4)
C(46A)	2317(10)	5660(9)	14460(9)	49(4)
F(42A)	3891(6)	3880(5)	14878(6)	64(3)
F(43A)	4431(6)	4894(6)	15722(6)	73(3)
F(44A)	3588(8)	6465(7)	15690(7)	94(4)
F(45A)	2180(8)	6955(6)	14849(7)	89(3)
F(46A)	1609(6)	5933(5)	14049(6)	63(2)
C(51A)	2235(10)	4805(9)	12882(9)	46(4)
C(52A)	2899(11)	5264(10)	12550(9)	55(4)
C(53A)	2950(12)	5681(11)	11762(11)	67(5)
C(54A)	2277(13)	5649(11)	11304(11)	72(5)
C(55A)	1629(12)	5221(11)	11592(11)	66(5)
C(56A)	1605(11)	4819(9)	12369(9)	52(4)
F(52A)	3589(6)	5289(6)	12968(5)	66(3)
F(53A)	3611(8)	6096(8)	11452(6)	102(4)
F(54A)	2325(9)	6053(8)	10530(6)	113(4)
F(55A)	999(7)	5181(8)	11136(6)	96(4)
F(56A)	941(6)	4399(6)	12634(6)	75(3)

Table 4 (*Continued*)

Atom	*x*	*y*	*z*	$U_{(eq)}$
B(1)	5332(6)	1269(7)	1938(6)	60(5)
F(1)	5750(12)	1798(11)	2243(11)	178(8)
F(2)	5905(7)	921(7)	1404(6)	94(4)
F(3)	5107(13)	790(12)	2649(9)	82(6)
F(3′)	5078(22)	550(14)	2369(19)	111(12)
F(4)	4755(11)	1881(10)	1572(11)	76(6)
F(4′)	4609(10)	1541(14)	1540(12)	54(6)
B(2)	8810(10)	5019(8)	3432(8)	89(8)
F(5)	9125(9)	4338(7)	3953(9)	137(6)
F(6)	9002(26)	4740(24)	2722(15)	149(13)
F(6′)	8084(16)	4797(19)	3201(19)	157(11)
F(7)	8026(13)	5405(18)	3655(18)	103(9)
F(7′)	8437(16)	5608(12)	3868(13)	106(7)
F(8)	9431(17)	5519(17)	3429(20)	120(10)
F(8′)	9205(15)	5340(15)	2717(11)	108(7)
O(1)	2391(18)	7301(16)	12488(16)	82(7)
C(14)	1859(28)	7736(24)	12301(24)	74(11)
C(15)	1119(42)	7543(40)	12231(41)	184(28)
C(16)	1423(41)	8087(37)	12996(34)	159(24)

3. Conclusion

The reaction between $[(\eta^5\text{-}C_5Me_4Et)RhCl(\mu\text{-}Cl)]_2$ and dfppe proceeds similarly to that between $[(\eta^5\text{-}C_5Me_5)RhCl(\mu\text{-}Cl)]_2$ and dfppe [10,11]. Although the C–F bond activation is regiospecific, activation of the C–H bonds of the C_5Me_4Et ligand is not. Presumably, cleavage of C–H bonds on alkyl groups in a 1,3-disposition occurs, but the spectroscopic data indicate that C–H bonds of all the cyclopentadienyl methyl and methylene groups can be activated to give a mixture of isomers. The reactions show little discernible selectivity in the activation of these bonds. Although there was no evidence for the activation of the alkyl methyl C–H bonds this can not be ruled out. The reactions also showed no stereospecificity as to which methylene C–H bond was activated, since both isomers **IV** and **V** of cation **3** were identified. The similarity of the relative intensities of the NMR resonances of the products of the reactions between $[(\eta^5\text{-}C_5Me_4Et)RhCl(\mu\text{-}Cl)]_2$ and dfppe carried out in benzene and ethanol, and the thermolysis of **4b**, suggest that the reactions proceed via the same mechanism, i.e. formation of the cation **4** followed by sequential C–F and C–H bond activation and C–C bond formation to give **5** then **3**.

4. Experimental details

4.1. General procedures

^{1}H-, ^{19}F- and ^{31}P-NMR spectra were recorded on Bruker DRX400, AM300 or ARX250 spectrometers. ^{1}H-NMR spectra were referenced using the residual protio solvent resonance relative to tetramethylsilane

($\delta = 0$), ^{19}F- and ^{31}P-NMR spectra externally to $CFCl_3$ and 85% H_3PO_4 respectively, using the high frequency positive convention. ^{19}F-NMR spectra of salts containing BF_4^-, the fluorine atoms of which have a relatively high values of T_1, were recorded with a relaxation delay of 10 s. All chemical shifts (δ) are quoted in ppm and coupling constants in Hz. Abbreviations used in multiplicities are: s, singlet; d, doublet; t, triplet; q, quartet; m, multiplet; br denotes a signal broadened due to a fluxional process. Elemental analyses were performed by Butterworths. Positive-ion FAB mass spectra were obtained on a Kratos Concept ^{1}H mass spectrometer.

4.2. Reagents

C_5Me_4EtH, $RhCl_3 \cdot xH_2O$, $[(\eta^5\text{-}C_5Me_5)RhCl(\mu\text{-}Cl)]_2$ (Aldrich) and $PPh_2(C_6F_5)$, $PPh(C_6F_5)_2$, $P(C_6F_5)_3$ and $(C_6F_5)_2PCH_2CH_2P(C_6F_5)_2$ (Fluorochem) were used as supplied. $[(\eta^5\text{-}C_5Me_4Et)RhCl(\mu\text{-}Cl)]_2$ was prepared as described for $[(\eta^5\text{-}C_5Me_5)RhCl(\mu\text{-}Cl)]_2$ [16].

4.3. Preparations

4.3.1. Reaction between $[(\eta^5\text{-}C_5Me_4Et)RhCl(\mu\text{-}Cl)]_2$ and dfppe in benzene

A slurry of $[(\eta^5\text{-}C_5Me_4Et)RhCl(\mu\text{-}Cl)]_2$ (0.16 g, 0.25 mmol) and dfppe (0.39 g, 0.51 mmol) in benzene (65 cm^3) was refluxed under nitrogen for 10.5 h. The resulting yellow solution was concentrated to ca. 20 cm^3 by rotary evaporation and light petroleum (b.p. 100–120°C) added to precipitate **3a** as a yellow powder, which was filtered off, washed with light petroleum (b.p. 40–60°C) and dried in vacuo. Yield 0.29 g (55%). FAB MS m/z: 1005 (M^+), 969 ($[M-Cl-H]^+$). The tetrafluoroborate salt, **3b**, was prepared by anion metathesis. Typically, a sample of **3a** in dichloromethane (ca. 20 cm^3) was added to a large excess of NH_4BF_4 in methanol (ca. 150 cm^3) and the mixture stirred for 2 h. The solvent was removed by rotary evaporation and the product extracted in dichloromethane (50 cm^3) and filtered. The solvent was removed by rotary evaporation to afford **3b**, which was recrystallized from acetone. FAB MS m/z: 1005 ($[M-BF_4]^+$), 969 ($[M-BF_4-Cl-H]^+$). Anal. Found: C, 41.4; H, 2.1; P, 5.5. $C_{37}H_{19}BClF_{22}P_2Rh \cdot 1/2\{(CH_3)_2CO\}$ Calc: C, 41.2; H, 2.0; P, 5.5%.

4.3.2. Reaction between $[(\eta^5\text{-}C_5Me_4Et)RhCl(\mu\text{-}Cl)]_2$ and dfppe in ethanol

A slurry of $[(\eta^5\text{-}C_5Me_4Et)RhCl(\mu\text{-}Cl)]_2$ (0.06 g, 0.09 mmol) and dfppe (0.13 g, 0.18 mmol) in ethanol (50 cm^3) was refluxed under nitrogen for 2 h. The solvent was removed by rotary evaporation and NH_4BF_4 (ca. 1 g) and acetone (70 cm^3) was added. After stirring for 2 h. the solvent was removed by rotary evaporation and the solid extracted with dichloromethane (70 cm^3) and filtered. Removal of the solvent by rotary evaporation afforded 0.135 g of a yellow solid comprising **3b**, **4b** and **5b**.

4.3.3. Preparation of $[(\eta^5\text{-}C_5Me_4Et)RhCl\{(C_6F_5)_2PCH_2CH_2P(C_6F_5)_2\}]^+ \cdot BF_4^-$ (4b)

The salt NH_4BF_4 (0.10 g, 0.95 mmol) was added to $[(\eta^5\text{-}C_5Me_4Et)RhCl(\mu\text{-}Cl)]_2$ (0.10 g, 0.15 mmol) in methanol (50 cm^3) and the mixture stirred for 10 min. Dfppe (0.23 g, 0.30 mmol) in dichloromethane (30 cm^3) was added and the mixture stirred for 2.5 h. The solvent was removed by rotary evaporation and the product extracted into dichloromethane (2×50 cm^3).

Table 5
Selected interatomic distances (Å) and angles (°) for $[(\eta^5\text{-}C_5Me_4Et)RhCl\{(C_6F_5)_2PCH_2CH_2P(C_6F_5)_2\}]^+ \cdot BF_4^- \cdot \{(CH_3)_2CO\}_{0.25}$ (**4b** $\cdot \{(CH_3)_2CO\}_{0.25}$)

Bond lengths			
Rh(1)–Cl(1)	2.383(4)	Rh(2)–Cl(2)	2.377(4)
Rh(1)–P(1)	2.345(4)	Rh(2)–P(3)	2.353(4)
Rh(1)–P(2)	2.380(4)	Rh(2)–P(4)	2.342(4)
Rh(1)–C(3)	2.247(13)	Rh(2)–C(3A)	2.215(14)
Rh(1)–C(4)	2.276(13)	Rh(2)–C(4A)	2.188(14)
Rh(1)–C(5)	2.211(12)	Rh(2)–C(5A)	2.253(12)
Rh(1)–C(6)	2.224(13)	Rh(2)–C(6A)	2.226(13)
Rh(1)–C(7)	2.179(14)	Rh(2)–C(7A)	2.241(14)
P(1)–C(1)	1.828(13)	P(3)–C(1A)	1.821(13)
P(1)–C(21)	1.856(14)	P(3)–C(21A)	1.82(2)
P(1)–C(31)	1.86(2)	P(3)–C(31A)	1.85(2)
P(2)–C(2)	1.820(13)	P(4)–C(2A)	1.835(14)
P(2)–C(41)	1.824(14)	P(4)–C(41A)	1.850(14)
P(2)–C(51)	1.818(14)	P(4)–C(51A)	1.84(2)
C(1)–C(2)	1.52(2)	C(1A)–C(2A)	1.51(2)
Non-bonded distances			
C(10)···F(42)	2.910(19)	C(9A)···C(42A)	3.263(20)
C(10)···F(52)	3.181(18)	C(11A)···F(26A)	3.108(20)
C(11)···F(22)	3.170(17)	C(11A)···F(32A)	2.997(17)
C(11)···F(42)	3.186(16)	C(12A)···F(32A)	3.137(21)
C(12)···F(36)	3.241(19)	C(13A)···F(42A)	3.165(18)
C(13)···F(36)	3.153(20)	C(13A)···F(52A)	3.153(20)
Bond angles			
Cl(1)–Rh(1)–P(1)	84.27(13)	Cl(2)–Rh(2)–P(3)	79.23(14)
Cl(1)–Rh(1)P(2)	85.59(13)	Cl(2)–Rh(2)–P(4)	90.65(13)
P(1)–Rh(1)–P(2)	82.97(13)	P(3)–Rh(2)–P(4)	82.75(13)
Rh(1)–P(1)–C(1)	109.7(4)	Rh(2)–P(3)–C(1A)	105.3(5)
Rh(1)–P(1)–C(21)	123.9(5)	Rh(2)–P(3)–C(21A)	112.7(5)
Rh(1)–P(1)–C(31)	111.3(5)	Rh(2)–P(3)–C(31A)	128.5(5)
C(1)–P(1)–C(21)	98.6(6)	C(1A)–P(3)–C(21A)	107.4(7)
C(1)–P(1)–C(31)	108.1(7)	C(1A)–P(3)–C(31A)	102.1(7)
C(21)–P(1)–C(31)	103.9(6)	C(21A)–P(3)–C(31A)	99.2(7)
Rh(1)–P(2)–C(2)	104.2(5)	Rh(2)–P(4)–C(2A)	110.1(5)
Rh(1)–P(2)–C(41)	117.7(5)	Rh(2)–P(4)–C(41A)	123.7(5)
Rh(1)–P(2)–C(51)	123.1(5)	Rh(2)–P(4)–C(51A)	113.3(5)
C(2)–P(2)–C(41)	107.8(7)	C(2A)–P(4)–C(41A)	100.1(7)
C(2)–P(2)–C(51)	101.5(6)	C(2A)–P(4)–C(51A)	106.3(7)
C(41)–P(2)–C(51)	100.7(7)	C(41A)–P(4)–C(51A)	101.5(6)
P(1)–C(1)–C(2)	112.(9)	P(3)–C(1A)–C(2A)	112.9(10)
P(2)–C(2)–C(1)	111.3(9)	P(4)–C(2 A)–C(1A)	112.8(9)

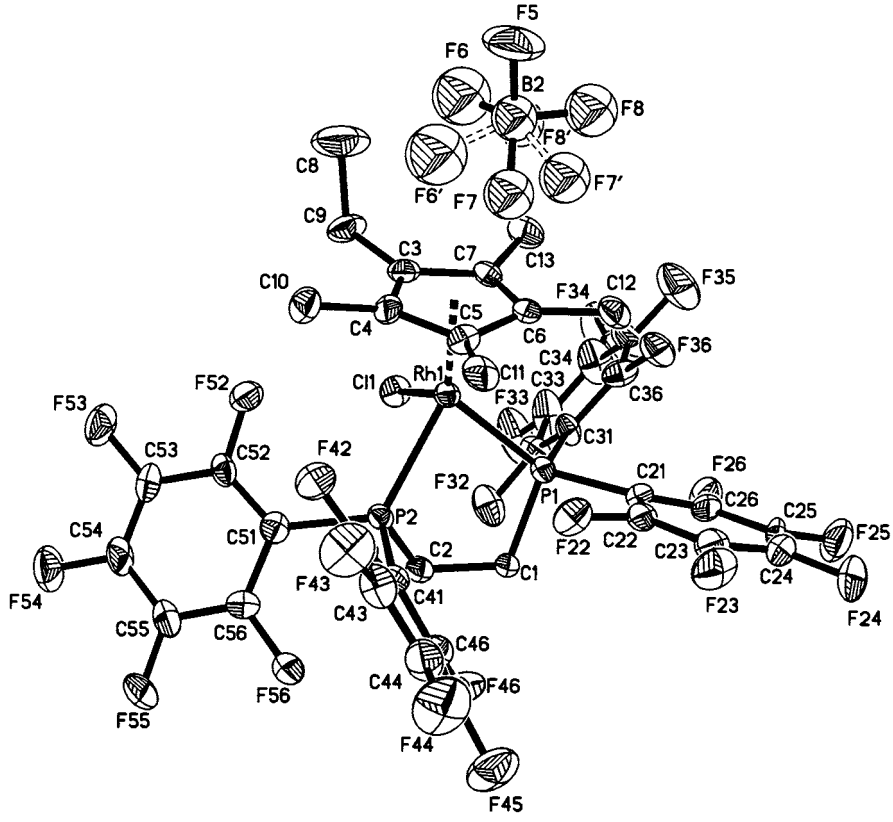

Fig. 6. Molecular structure of one of the independent ion pairs of $[(\eta^5\text{-}C_5Me_4Et)RhCl\{(C_6F_5)_2PCH_2CH_2P(C_6F_5)_2\}]^+ \cdot BF_4^-$ (**4b**). Displacement ellipsoids are shown a the 30% probability level. All hydrogen atoms are omitted for clarity.

Concentration by rotary evaporation and addition of light petroleum precipitated **4b** as a yellow solid, which was filtered off, washed with light petroleum (bp 40–60°C) and dried. Yield 0.21 g (62%). ^{1}H [$(CD_3)_2CO$, 300.14 MHz]: 3.40 (m, 4H, PCH_2), 2.23 (q, $^3J_{H-H}$ 7.5 Hz, 2H, CH_2CH_3), 1.77 (m, 12H, C_5CH_3), 1.31 (t, $^3J_{H-H}$ 7.5 Hz, 3H, CH_2CH_3). ^{19}F [$(CD_3)_2CO$, 282.41 MHz]: −124.29 (br s, 4F, F_{ortho}), −127.43 (d, $^3J_{F-F}$ 9.7 Hz, 4F, F_{ortho}), −144.92 (t, $^3J_{F-F}$ 21.2 Hz, 2F, F_{para}), −146.14 (t, $^3J_{F-F}$ 20.5 Hz, 2F, F_{para}), −150.90 and −150.95 (1:4) (4F, BF_4^-), −158.26 (dd, $^3J_{Fortho-Fmeta}$ ca. $^3J_{Fmeta-Fpara}$ 20.2, 4F, F_{meta}), −160.27 (dd, $^3J_{Fortho-Fmeta} \approx {}^3J_{Fmeta-Fpara}$ 19.4, 4F, F_{meta}). ^{31}P{^{1}H} [$(CD_3)_2CO$, 121.50 MHz]: 34.2 (dm, $^1J_{Rh-P}$ 152 Hz). FAB MS m/z: 1045 ($[M-BF_4]^+$), 1010 ($[M-BF_4-Cl]^+$). Anal. Found: C, 40.8; H, 2.2; P, 4.3. $C_{37}H_{21}BClF_{24}P_2Rh$ Calc.: C, 39.2; H, 1.9; P, 5.4%. (Satisfactory analysis could not be obtained due to contamination by C–F bond activated species. Characterization was based on the spectroscopic data and by comparison with complex **2b** [11]).

4.3.4. Preparation of $(\eta^5\text{-}C_5Me_5)RhCl_2\{PPh_2(C_6F_5)\}$

A slurry of $[(\eta^5\text{-}C_5Me_5)RhCl(\mu\text{-}Cl)]_2$ (0.06 g, 0.10 mmol) and $PPh_2(C_6F_5)$ (0.07 g, 0.20 mmol) in benzene (160 cm^3) was refluxed under nitrogen for 3 h. After cooling and addition of light petroleum (b.p. 100–120°C), concentration by rotary evaporation and addition of more light petroleum precipitated **6** as a red solid. Yield 0.055 g (42%). ^{1}H ($CDCl_3$, 300.14 MHz): 7.86 (m, 4H, Ph), 7.41 (m, 6H, Ph), 1.30 (d, $^4J_{P-H}$ 2.2, 15H, CH_3). ^{19}F ($CDCl_3$, 282.41 MHz): −120.43 (dm, $^3J_{Fortho-Fmeta}$ 16.8 Hz, 2F, F_{ortho}), −148.29 (m, 1F, F_{para}), −160.11 (m, 2F, F_{meta}). ^{31}P{^{1}H} ($CDCl_3$, 121.50 MHz): 18.8 (dm, $^1J_{Rh-P}$ 149 Hz). FAB MS m/z: 660 ($[M-H]^+$), 625 ($[M-Cl-H]^+$), 590 ($[M-2Cl-H]^+$), 580 ($[M-C_6H_5-H]^+$). Anal. Found: C, 51.4; H, 3.7; P, 4.7. $C_{28}H_{25}Cl_2F_5PRh$ Calc.: C, 50.9; H, 3.8; P, 4.7%.

4.4. X-ray crystal structure determination

Crystals of salt **4b** suitable for X-ray structure determination were grown from acetone. The structure was determined on a Siemens P4 diffractometer. Crystallographic data are presented in Table 3 and atomic coordinates and isotropic displacement parameters are given in Table 4. Accurate unit cell parameters were determined by least-squares refinement of the optimised setting angles of 28 reflections in the range $5.5 \leq \theta \leq 12.5°$. Three standard check reflections, monitored every 100 reflections, indicated no crystal decay. A semi-empirical correction, based on the ψ scan data,

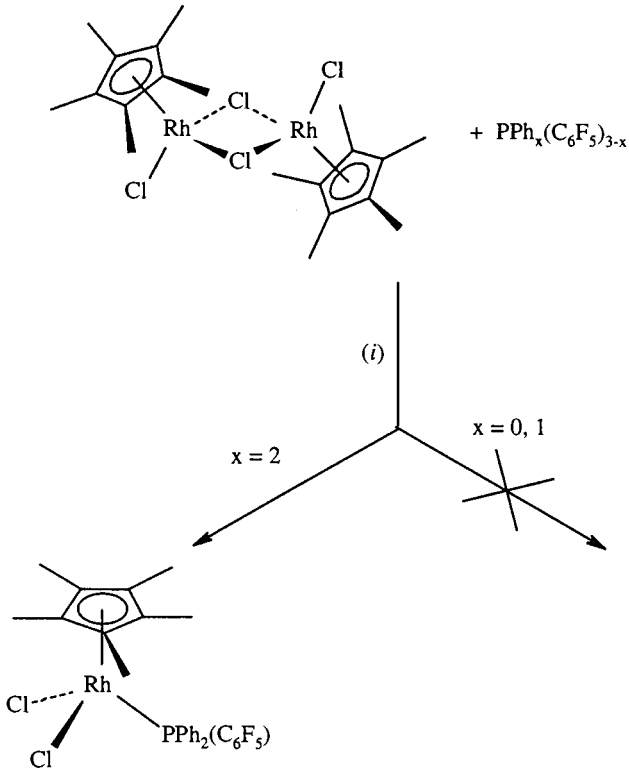

Scheme 3. (i) benzene, heat.

was applied to the data (maximum and minimum transmission factors 0.950 and 0.693, respectively), and the data were corrected for Lorentz and polarization effects.

The structure was solved by direct methods using the PATT option of SHELXTL-pc [17] and refined by full matrix least squares. Hydrogen atoms were included in calculated positions (C–H 0.95 Å) with a single fixed isotropic displacement parameter ($U_{iso} = 0.08$ Å^3). The boron atoms and carbons atoms other than the methyl and ethyl atoms of the C_5Me_4Et ligands were refined with isotropic displacement parameters. All other non-hydrogen atoms were refined with anisotropic displacement parameters. Due to program constraints of 800 parameters to be refined, the C_6F_5 rings were refined as rigid groups with x, y and z of all other atoms riding on the pivot atom. An analysis of the weighting scheme over $|F_0|$ and $(\sin\theta)/\lambda$ was satisfactory. The highest residual electron density peaks were close to the boron atoms (ca. 1.42 Å) consistent with disorder typical of BF_4^- anions.

Acknowledgements

We thank F_2 Chemicals (GCS) and the Royal Society (EGH) for support.

References

[1] (a) J.L. Kiplinger, T.G. Richmond, C.E. Osterberg, Chem. Rev. 94 (1994) 373. (b) G.C. Saunders, Angew. Chem., Int. Ed. Engl. 35 (1996) 2615. (c) J. Burdeniuc, B. Jedlicka, R.H. Crabtree, Chem. Ber. 130 (1997) 145.
[2] (a) T.G. Richmond, C.E. Osterberg, A.M. Arif, J. Am. Chem. Soc. 109 (1987) 8091. (b) C.E. Osterberg, M.A. King, A.M. Arif, T.G. Richmond, Angew. Chem. Int. Ed. Engl. 29 (1990) 888. (c) B.L. Lucht, M.J. Poss, M.A. King, T.G. Richmond, J. Chem. Soc. Chem. Commun. (1991) 400.
[3] (a) C.M. Anderson, R.J. Puddephat, G. Ferguson, A.J. Lough, J. Chem. Soc. Chem. Commun. (1989) 1297. (b) C.M. Anderson, M. Crespo, G. Ferguson, A.J. Lough, R.J. Puddephat, Organometallics 11 (1992) 1177. (c) M. Crespo, M. Martinez, J. Sales, J. Chem. Soc. Chem. Commun. (1992) 822. (d) M. Crespo, M. Martinez, J. Sales, Organometallics 12 (1993) 4297. (e) M. Crespo, X. Solans, M. Font-Bardía, Organometallics 14 (1995) 355. (f) M. Crespo, M. Martinez, E. de Pablo, J. Chem. Soc. Dalton Trans. (1997) 1231.
[4] L.J. Procopio, P.J. Carroll, D.H. Berry, J. Am. Chem. Soc. 116 (1994) 177.
[5] M.L.H. Green, J. Haggitt, C.P. Mehnert, J. Chem. Soc. Chem. Commun. (1995) 1853.
[6] M. Aizenberg, D. Milstein, J. Am. Chem. Soc. 117 (1995) 8674.
[7] R.M. Ceder, J. Granell, G. Muller, M. Font-Bardía, X. Solans, Organometallics 14 (1995) 5544.
[8] J.L. Kiplinger, T.G. Richmond, J. Chem. Soc. Chem. Commun. (1996) 1115.
[9] J. Burdeniuc, R.H. Crabtree, J. Am. Chem. Soc. 118 (1996) 2525.
[10] M.J. Atherton, J. Fawcett, J.H. Holloway, E.G. Hope, A. Karaçar, D.R. Russell, G.C. Saunders, J. Chem. Soc. Chem. Commun. (1995) 191.
[11] M.J. Atherton, J. Fawcett, J.H. Holloway, E.G. Hope, A. Karaçar, D.R. Russell, G.C. Saunders, J. Chem. Soc. Dalton Trans. (1996) 3215.
[12] L.P. Barthel-Rosa, V.J. Catalano, J.H. Nelson, J. Chem. Soc. Chem. Commun. (1995) 1629.
[13] L.P. Barthel-Rosa, V.J. Catalano, K. Maitra, J.H. Nelson, Organometallics 15 (1996) 3924.
[14] A. Bondi, J. Phys. Chem. 68 (1964) 441.
[15] M.J. Atherton, J. Fawcett, A.P. Hill, J.H. Holloway, E.G. Hope, D.R. Russell, G.C. Saunders, R.M.J. Stead, J. Chem. Soc. Dalton Trans. (1997) 1137.
[16] C. White, A. Yates, P.M. Maitlis, Inorg. Synth. 29 (1992) 228.
[17] G.M. Sheldrick, SHELXTL-PC, Release 4.2, Siemens Analytical X-Ray Instruments, Madison, WI, 1991.